DALTON

Syntheses, crystal structures and magnetic properties of $[Ni_2(C_2O_4)(tren)_2][ClO_4]_2$ and $[Ni_2(C_4O_4)(tren)_2(H_2O)_2][ClO_4]_2$ [tren = tris(2-aminoethyl)amine]

Isabel Castro,[a] M. Luisa Calatayud,[a] Jorunn Sletten,*[,b] Francesc Lloret[a] and Miguel Julve*[,a]

[a] *Departament de Química Inorgànica, Facultat de Química de la Universitat de València, c/ Dr. Moliner 50, 46100 Burjassot* (*València*), *Spain*
[b] *Kjemisk Institutt, Universitetet i Bergen, N-5007 Bergen, Norway*

Two dinuclear nickel(II) complexes $[Ni_2(C_2O_4)(tren)_2][ClO_4]_2$ **1** and $[Ni_2(C_4O_4)(tren)_2(H_2O)_2][ClO_4]_2$ **2** [tren = tris(2-aminoethyl)amine, $C_2O_4^{2-}$ = oxalate dianion and $C_4O_4^{2-}$ = dianion of 3,4-dihydroxycyclobut-3-en-1,2-dione (squaric acid)] have been synthesized and characterized by single-crystal X-ray diffraction. Their structures consist of dinuclear nickel(II) cations and unco-ordinated perchlorate anions. The nickel environment is distorted octahedral NiN_4O_2 in both complexes: four nitrogen atoms of the tren group acting as a tetradentate ligand and two oxygen atoms of oxalate (**1**) or a water molecule and a squarate oxygen (**2**) comprise the co-ordination. The oxalate acts as a bis(chelating) ligand whereas the squarate adopts a μ-1,2-bis(monodentate) co-ordination mode. The intradimer metal–metal separation is 5.413(1) and 6.224(1) Å in **1** and **2**, respectively. The co-ordinated water molecule in **2** forms an intramolecular hydrogen bond to an unco-ordinated squarate-oxygen atom. Variable-temperature susceptibility measurements revealed the occurrence of relatively strong (**1**) and weak (**2**) intramolecular antiferromagnetic coupling, the relevant parameters being $J = -28.8$ cm^{-1} and $g = 2.16$ for **1** and $J = -0.4$ cm^{-1} and $g = 2.15$ for **2** (J being the exchange parameter in the isotropic spin Hamiltonian $\hat{H} = -J\hat{S}_A\cdot\hat{S}_B$). A comparative study of the ability of oxalate and squarate groups to mediate electronic interactions in the structurally characterized oxalato- and squarato-bridged nickel(II) complexes was carried out.

The reactions of oxalate (dianion of oxalic acid, $H_2C_2O_4$) and squarate (dianion of 3,4-dihydroxycyclobut-3-en-1,2-dione, $H_2C_4O_4$) with nickel(II) ions yield polymeric compounds of formula $[Ni(C_2O_4)(H_2O)_2]$ and $[Ni(C_4O_4)(H_2O)_2]$.[1,2] The structure of the former consists of chains of oxalate-bridged nickel(II) ions whereas that of the latter is made up of layers of squarato-O^1,O^2,O^3,O^4-bridged nickel(II) ions. In both cases the octahedral co-ordination of the metal ion is completed by two water molecules in *trans* position. The different co-ordination modes adopted by oxalate [bis(chelating)] and squarate (tetramonodentate) towards nickel(II) can be explained by geometrical effects: the value of the bite parameter for squarate [bite distance/M–O (squarate)][3,4] in its complexes with first-row transition-metal ions is too large and so it adopts mono- or polymono-dentate co-ordination modes. Nevertheless, the chelating and bis(chelating) co-ordination modes of squarate are possible in its complexes with heavier metal ions (alkali- and rare-earth-metal cations)[5,6] due to the reduction of the bite parameter. These modes are also possible for thiosquarates due to the large bonding radius of sulfur (1,2-dithio-, 1,3-dithio- and 1,2,3,4-tetrathio-squarate).[7–9]

The use of blocking ligands allows the co-ordination chemist to control polymerization and renders easier nuclearity tailoring of desired polynuclear compounds. In the case of nickel(II), cyclic and acyclic polydentate amines appear the most common terminal ligands in oxalato-bridged dinuclear complexes.[10] However, the recent structural determination of the compound $[H_3dien]_2[Ni_2(C_2O_4)_5]\cdot 12H_2O$,[10k] where the oxalate is both bridging and peripheral (dien = diethylenetriamine), offers new perspectives to the synthetic chemist. Magnetostructural data concerning the oxalato-bridged nickel(II) complexes have revealed that the magnetic coupling J, which varies from −22 to −39 cm^{-1}, is strongly dependent on the nature of the donor atoms of the terminal ligands.[10k] In the case of squarato-nickel(II) complexes, apart from the sheet-like polymer $[Ni(C_4O_4)(H_2O)_2]$, only two chain compounds $[Ni(C_4O_4)(Him)(H_2O)_2]$[11] (Him = imidazole) and $[Ni(C_4O_4)(bipy)(H_2O)_2]\cdot 2H_2O$[12] (bipy = 2,2′-bipyridyl) have been structurally characterized. They are made up of squarato-O^1,O^3(imidazole)- and squarato-O^1,O^2(bipyridyl)-bridged nickel(II) ions. Magnetic susceptibility measurements showed that the exchange interaction between the nickel(II) ions in this series is very weak in contrast to the situation found in the related oxalato compounds.

In the present work we show that the use of tetradentate tris(2-aminoethyl)amine (tren) as peripheral group allows the preparation of two dinuclear nickel(II) complexes of formula $[Ni_2(C_2O_4)(tren)_2][ClO_4]_2$ **1** and $[Ni_2(C_4O_4)(tren)_2(H_2O)_2][ClO_4]_2$ **2**. This contribution is devoted to their syntheses, spectroscopic and magnetostructural characterization.

Experimental

Materials

The compounds tren, nickel(II) perchlorate hexahydrate, sodium oxalate and squaric acid were obtained from commercial sources and used as received. Elemental analyses (C, H, N, Cl) were conducted by the Microanalytical Service of the Universidad Autónoma de Madrid.

Synthesis

CAUTION: perchlorate salts of metal complexes with organic ligands are potentially explosive. Only a small amount of material should be prepared and handled with care.

$[Ni_2(C_2O_4)(tren)_2][ClO_4]_2$ 1. This complex was prepared by adding an aqueous solution of sodium oxalate [0.134 g (1 mmol) dissolved in the minimum volume of warm water] to an aqueous solution (50 cm^3) of $[Ni(tren)][ClO_4]_2$ {$[Ni(H_2O)_6][ClO_4]_2$ (0.7314 g, 2 mmol) and tren (0.292 g, 2 mmol)}. The addition of oxalate is accompanied by a change from blue to violet and by subsequent formation of a violet microcrystalline solid of **1** which was filtered off, washed with cold water and

dried *in vacuo*. Mauve thin plates of **1** suitable for X-ray analysis were obtained from the remaining solution by slow evaporation at room temperature. Yield 92% (Found: C, 24.25; H, 5.2; Cl, 9.95; N, 15.85. Calc. for $C_{14}H_{36}Cl_2N_8Ni_2O_{12}$: C, 24.15; H, 5.15; Cl, 10.2; N, 16.1%).

$[Ni_2(C_4O_4)(tren)_2(H_2O)_2][ClO_4]_2$ 2. This complex was prepared by adding an aqueous solution of lithium squarate [$H_2C_4O_4$ (0.114 g, 1 mmol) and $LiOH \cdot H_2O$ (0.0839 g, 2 mmol) dissolved in the minimum volume of warm water] to an aqueous solution (25 cm^3) of [Ni(tren)][ClO_4]$_2$ {[$Ni(H_2O)_6$][ClO_4]$_2$ (0.7314 g, 2 mmol) and tren (0.292 g, 2 mmol)}. As in the preceding synthesis, the addition of squarate was accompanied by a change from blue to violet and by formation of a small amount of solid which was discarded. Mauve prisms of **2** suitable for X-ray analysis were obtained from the remaining solution by slow evaporation at room temperature. Yield about 90% (Found: C, 25.2; H, 5.2; Cl, 9.1; N, 14.6. Calc. for $C_{16}H_{40}Cl_2N_8Ni_2O_{14}$: C, 25.4; H, 5.3; Cl, 9.35; N, 14.8%).

Physical techniques

Infrared spectra were recorded on a Perkin-Elmer 1750 FTIR spectrophotometer as KBr pellets in the 4000–300 cm^{-1} region and electronic spectra of aqueous solutions and Nujol mull samples on a Perkin-Elmer Lambda 9 spectrophotometer. The magnetic susceptibility of a polycrystalline sample was measured over the temperature range 10–300 (**1**) and 4.2–300 K (**2**) in a field of 1 T by using a fully automatized AZTEC DSM8 pendulum-type susceptometer equipped with a TBT continuous-flow cryostat and a Bruker BE15 electromagnet operating at 1.8 T. Mercury tetrakis(thiocyanato)cobaltate(II) was used as a susceptibility standard. Diamagnetic corrections for the constituent atoms were estimated from Pascal's constants[13] and found to be -257×10^{-6} (**1**) and -307×10^{-6} cm^3 mol^{-1} (**2**). Experimental susceptibilities were corrected for the temperature-independent paramagnetism (-100×10^{-6} cm^3 mol^{-1} per Ni^{II}).

Crystallography

X-Ray diffraction data of complexes **1** and **2** were collected at 21 °C with an Enraf-Nonius CAD-4 diffractometer using graphite-monochromatized Mo-Kα radiation (λ = 0.710 73 Å). Unit cell parameters were determined from least-squares refinement of the setting angles of 25 reflections with 2θ in the range 35–42°. A summary of the crystallographic data and structure refinement parameters is given in Table 1. Totals of 2340 (**1**) and 6880 (**2**) unique reflections were recorded within 2θ < 50 (**1**) and 2θ < 55° (**2**) using the ω–2θ scan technique. Three reference reflections monitored throughout each data collection showed no intensity loss for **1** and an average decrease of 6% for **2**. The data were corrected for Lorentz-polarization effects and for linear decay. Experimental absorption corrections based on ψ scans of seven reflections were carried out for both structures.

The structures were solved by direct methods[14] and successive Fourier syntheses. All non-hydrogen atoms were refined anisotropically. Hydrogen atoms were located in Fourier-difference and refined isotropically. The final full-matrix least-squares refinements on F, minimizing $\Sigma w(|F_o| - |F_c|)^2$, including 1893 (**1**) and 5173 (**2**) reflections with $I > 2\sigma$, adjusting 244 (**1**) and 540 (**2**) parameters, converged at R and R' indices of 0.035 and 0.040 for **1**, 0.034 and 0.040 for **2**. In the final difference maps the residual maxima and minima were 0.69 and −0.28 e $Å^{-3}$ for **1**, 0.46 and −0.11 e $Å^{-3}$ for **2**. All calculations were carried out with programs in the MOLEN system.[15] Neutral atomic scattering factors were used,[16] and anomalous scattering terms were included in F_c.[17] Selected bond distances and angles for compounds **1** and **2** are given in Tables 2 and 3, respectively.

Atomic coordinates, thermal parameters, and bond lengths and angles have been deposited at the Cambridge Crystallographic Data Centre (CCDC). See Instructions for Authors, *J. Chem. Soc., Dalton Trans.*, 1997, Issue 1. Any request to the CCDC for this material should quote the full literature citation and the reference number 186/370.

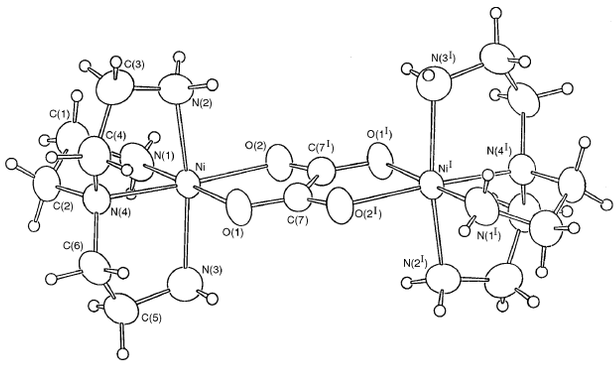

Fig. 1 The dinuclear unit $[Ni_2(C_2O_4)(tren)_2]^{2+}$ of complex **1** with the atomic numbering used. Thermal ellipsoids are plotted at the 70% probability level

Results and discussion

Structures

$[Ni_2(C_2O_4)(tren)_2][ClO_4]_2$ 1. The structure of complex **1** consists of centrosymmetric, oxalato-bridged $[Ni_2(C_2O_4)(tren)_2]^{2+}$ units (Fig. 1) and non-co-ordinated ClO_4^- counter ions. In the crystal there are weak hydrogen bonds between tren amine groups and oxalate in neighbouring molecules {2.947(4) and 3.152(5) Å for N(1)[H(13)] · · · O(2^{II}) (II $1 - x, -y, -z$) and N(2)[H(23)] · · · O(2^I), respectively; 167(4) and 164(4)° for N(1)–H(13) · · · O(2^{II}) and N(2)–H(23) · · · O(2^I), respectively} and weak interactions between amine and perchlorate oxygen atoms (N · · · O >3.2 Å).

The geometry about the nickel(II) ion is distorted octahedral with the co-ordination polyhedron defined by the four nitrogen atoms of the chelating tetradentate tren ligand and two oxygen atoms of bis(chelating) oxalate. The Ni–O (oxalate) distances are 2.112(2) and 2.049(2) Å for Ni(1)–O(1) and Ni(1)–O(2), respectively, whereas the Ni–N (terminal tren) bonds vary in the range 2.057(4)–2.145(3) Å and the Ni–N (central tren) is 2.081(3) Å. These distances agree with those observed in other oxalato-bridged[10] and tren-containing[8,18] nickel(II) complexes. Whereas the Ni–N (tren) bond to the tertiary nitrogen atom has been found to be either the longest or the shortest of the Ni–N bonds in $[Ni_2(1,3\text{-dtsq})(tren)_2]^{2+}$ (1,3-dtsq = 1,3-dithiosquarate dianion),[8] $[Ni_2(N_3)_2(tren)_2]^{2+}$,[18c] $[Ni_2(NCBH_3)_2(tren)_2]^{2+}$ [18d] and $[Ni_2(O_4C_6Cl_2)(tren)_2]^{2+}$,[18e] this bond is of intermediate length in the present compound, as well as in **2**. The best equatorial plane is comprised of atoms O(1), O(2), N(1) and N(4), the largest deviation from this mean plane being 0.050(2) Å for O(1). The metal atom does not exhibit any significant deviation from this plane. The value of the bite angle of the oxalate is 80.4(1)°, whereas those of the remaining five-membered rings at the metal atom subtended by the tetradentate tren ligand vary in the range 82.6(1)–84.0(1)°. The values at the carbon atoms bonded to the tertiary tren nitrogen [N(4)] reflect a normal tetrahedral geometry. The flexibility of the tren ligand allows two of the terminal nitrogen atoms [N(2) and N(3)] to be in *trans* positions. The normal trigonal geometry of the ligand appears to be responsible for the displacement of N(2) toward the N(4)–Ni–O(1) plane, the N(2)–Ni–N(3) bond angle being 163.7(1)°. The bridging oxalate is planar, and the nickel(II) ion is 0.044(1) Å out of this plane. The dihedral angle between the oxalate and equatorial mean planes is 3.6(5)°.

The intramolecular metal–metal distance across the oxalate bridge is 5.413(1) Å, slighly shorter than the shortest inter-

Table 1 Summary of crystal data[a] for $[Ni_2(C_2O_4)(tren)_2][ClO_4]_2$ **1** and $[Ni_2(C_4O_4)(tren)_2(H_2O)_2][ClO_4]_2$ **2**

Compound	**1**	**2**
Formula	$C_{14}H_{36}Cl_2N_8Ni_2O_{12}$	$C_{16}H_{40}Cl_2N_8Ni_2O_{14}$
M	696.82	756.87
Crystal system	Triclinic	Monoclinic
Space group	$P\bar{1}$ (no. 2)	$P2_1/c$ (no. 14)
a/Å	7.3408(6)	8.197(1)
b/Å	8.4551(9)	14.148(2)
c/Å	11.0098(9)	25.900(1)
α/°	101.289(8)	
β/°	90.208(7)	92.266(8)
γ/°	94.296(7)	
U/Å^3	668.1(2)	3001.4(9)
Z	1	4
D_c/g cm^{-3}	1.732	1.675
F(000)	362	1576
Crystal size/mm	0.36 × 0.15 × 0.06	0.53 × 0.28 × 0.21
μ(Mo-Kα)/mm^{-1}	1.6858	1.5124
Maximum, minimum transmission (%)[b]	99.8, 89.7	99.9, 94.0
Maximum 2θ/°	50	55
Scan range/°	1.10 + 0.35 tan θ	0.60 + 0.35 tan θ
Number unique reflections	2340	6880
Number used in refinement, N_o	1893	5173
Parameters refined, N_v	244	540
Extinction coefficient		1.68×10^{-8}
$R = (\Sigma\|\|F_o\| - \|F_c\|\|/\Sigma\|F_o\|)$	0.035	0.034
$R' = [\Sigma w(\|F_o\| - \|F_c\|)^2/\Sigma w\|F_o\|^2]^{\frac{1}{2}}$	0.040	0.040
$S = [\Sigma w(\|F_o\| - \|F_c\|)^2/(N_o - N_v)]^{\frac{1}{2}}$	1.531	1.938
k in weighting scheme	0.03	0.02

[a] Details in common: function minimized $\Sigma[w(|F_o| - |F_c|)^2]$, where $w = 4F_o^2/[\sigma_c^2 + (kF_o^2)^2]$ and σ_c is the standard deviation in F^2 based on counting statistics alone. [b] Empirical absorption correction based on ψ scans of seven reflections.

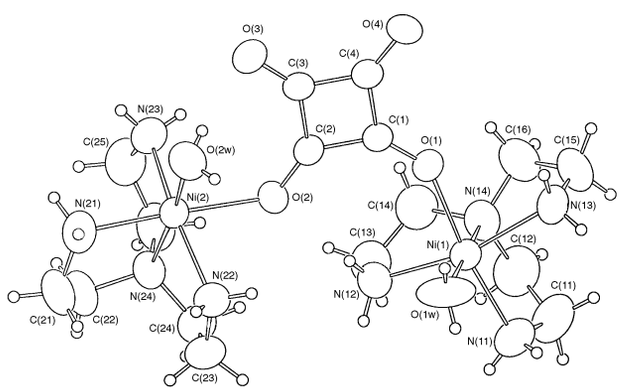

Fig. 2 The dinuclear unit $[Ni_2(C_4O_4)(tren)_2(H_2O)_2]^{2+}$ of complex **2** with the atomic numbering used. Thermal ellipsoids are plotted at the 70% probability level

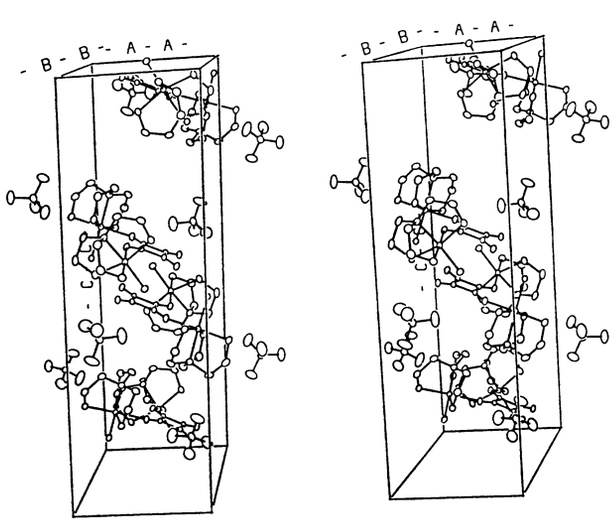

Fig. 3 Stereodrawing illustrating the crystal packing in compound **2**

molecular distance between metal ions [5.470(1) Å for Ni ··· Ni^{II}], other intermolecular metal–metal distances being all above 7 Å.

$[Ni_2(C_4O_4)(tren)_2(H_2O)_2][ClO_4]_2$ 2. The structure of complex **2** is comprised of squarato-O^1,O^2-bridged nickel(II) dinuclear units of formula $[Ni_2(C_4O_4)(tren)_2(H_2O)_2]^{2+}$ (Fig. 2) and non-co-ordinated perchlorate groups. Pairs of centrosymmetrically related molecules are arranged in such a way that the squarate groups overlap to a considerable extent with an interplanar spacing of 3.38 Å (Fig. 3).

The co-ordination geometries of the two crystallographically independent nickel(II) ions are distorted octahedral with Ni–O (squarate) 2.109(2) and 2.143(2) Å, Ni–O (water) 2.055(2) and 2.095(2) Å, Ni–N (terminal tren) 2.073(2)–2.125(2) Å, Ni–N (central tren) 2.074(2) and 2.083(2) Å. The Ni–O (water) bond lengths compare well with those observed in the compounds $[Ni(C_4O_4)(H_2O)_2]$ [2.060(9) Å],[2] $[Ni(C_4O_4)(Him)(H_2O)_2]$ [2.069(1) Å][11] and $[Ni(C_4O_4)(bipy)(H_2O)_2]\cdot 2H_2O$ [2.030(3) and 2.054(3)].[12] The average value of the Ni–O (squarate) bond distance (2.12 Å) is practically identical to those observed in the related imidazole and bipy derivatives, but somewhat longer than the corresponding bond in $[Ni(C_4O_4)(H_2O)_2]$ [2.085(16) Å]. The presence of strongly co-ordinated nitrogen donors (tren, Him and bipy) accounts for the lengthening of Ni–O (squarate) in this family. The angles subtended at the metal atom by the tetradentate tren ligand span the range 83.28(9)–84.43(9)° at Ni(1) and 83.48(9)–84.10(9)° at Ni(2). The values of the axial N(12)–Ni(1)–N(13) and N(22)–Ni(2)–N(23) bond angles are 163.54(9) and 163.36(9)°, respectively. The best equatorial plane around the metal atom is comprised of the atoms O(1), N(11), O(1w) and N(14) for Ni(1) [largest deviation from the mean plane 0.090(2) Å at N(14)] and by O(2), N(21), O(2w) and N(24) for Ni(2). The metal atoms are displaced 0.043(1) [Ni(1)] and 0.046(1) Å [Ni(2)] from the equatorial plane toward the axial N(12) [Ni(1)] and N(22) [Ni(2)] atoms.

The squarate group is planar [maximum deviation from the mean plane 0.017(2) Å at O(3)], and makes angles of 76.09(6)

Table 2 Selected interatomic distances (Å) and angles (°) for compound **1** with estimated standard deviations (e.s.d.s) in parentheses*

Nickel environment			
Ni–O(1)	2.112(2)	Ni–N(2)	2.145(3)
Ni–O(2)	2.049(2)	Ni–N(3)	2.115(4)
Ni–N(1)	2.057(4)	Ni–N(4)	2.081(3)
O(1)–Ni–O(2)	80.4(1)	O(2)–Ni–N(4)	173.8(1)
O(1)–Ni–N(1)	179.1(2)	N(1)–Ni–N(2)	94.2(2)
O(1)–Ni–N(2)	86.5(1)	N(1)–Ni–N(3)	93.6(2)
O(1)–Ni–N(3)	85.6(1)	N(1)–Ni–N(4)	83.9(1)
O(1)–Ni–N(4)	95.6(1)	N(2)–Ni–N(3)	163.7(1)
O(2)–Ni–N(1)	100.2(1)	N(2)–Ni–N(4)	82.6(1)
O(2)–Ni–N(2)	92.3(1)	N(3)–Ni–N(4)	84.0(1)
O(2)–Ni–N(3)	100.3(1)		
Oxalate ligand			
O(1)–C(7)	1.247(4)	O(2)–C(7^{I})	1.256(4)
C(7)–C(7^{I})	1.561(7)		
Ni–O(1)–C(7)	112.3(2)	O(1)–C(7)–C(7^{I})	116.6(4)
Ni–O(2)–C(7^{I})	113.8(2)	O(2)–C(7^{I})–C(7)	116.9(4)
O(1)–C(7)–O(2^{I})	126.5(3)		
tren ligands			
N(1)–C(1)	1.465(6)	N(4)–C(6)	1.481(5)
N(2)–C(3)	1.469(6)	C(1)–C(2)	1.534(6)
N(3)–C(5)	1.474(6)	C(3)–C(4)	1.518(6)
N(4)–C(2)	1.486(5)	C(5)–C(6)	1.513(6)
N(4)–C(4)	1.482(5)		
Ni–N(1)–C(1)	108.1(3)	C(4)–N(4)–C(6)	112.4(3)
Ni–N(2)–C(3)	109.4(3)	N(1)–C(1)–C(2)	109.3(3)
Ni–N(3)–C(5)	108.2(3)	N(4)–C(2)–C(1)	112.2(3)
Ni–N(4)–C(2)	109.5(2)	N(2)–C(3)–C(4)	110.3(3)
Ni–N(4)–C(4)	104.6(2)	N(4)–C(4)–C(3)	110.5(3)
Ni–N(4)–C(6)	105.1(2)	N(3)–C(5)–C(6)	109.8(3)
C(2)–N(4)–C(4)	113.1(3)	N(4)–C(6)–C(5)	110.1(3)
C(2)–N(4)–C(6)	111.6(3)		

*Symmetry code: I $-x, -y, -z$.

and 36.24(7)° with the equatorial O(1), N(11), O(1w), N(14) and O(2), O(2w), N(21), N(24) mean planes. The C–C bond lengths [1.469(3)–1.450(3) Å] are similar to those found in the related imidazole [1.470(2) and 1.463(2) Å] and bipy compounds [1.471(6)–1.448(6) Å], but somewhat smaller than the value reported for $[Ni(C_4O_4)(H_2O)_2]$ [1.487(16) Å]. In the case of squaric acid one of the C–C bond lengths is significantly shorter [1.409(1) Å].[19] The O–C–C angles vary in the range 138.0(2)–131.8(2)°, whereas the C–C–C angles are very close to 90°. The nickel atoms are significantly displaced from the least-squares plane through squarate [0.251(1) and 0.433(1) Å for Ni(1) and Ni(2), respectively]. The squarate group forms intramolecular hydrogen bonds to one co-ordinated water molecule [O(3) · · · O(2w) 2.687(3) Å] and one amine group, the latter being a rather weak interaction [O(2) · · · N(12) 3.112(3) Å]. Atoms O(1) and O(4) do not form corresponding contacts. This difference between the two halves of the squarate is related to the differences in dihedral angles between the squarate and the equatorial planes of the two nickel atoms. A number of intermolecular hydrogen bonds occur between co-ordinated water, amine tren groups, squarate and perchlorate oxygen atoms.

The intramolecular Ni(1) · · · Ni(2) distance is 6.224(1) Å whereas the shortest intermolecular distances between metal ions are 6.500(1) [Ni(1) · · · Ni(2^{I}); I $1-x, 1-y, 1-z$] and 6.791(1) Å [Ni(1) · · · Ni(2^{II}); II $-x, 1-y, 1-z$]. Other intermolecular metal–metal distances are all above 7 Å.

Infrared and electronic spectra

The infrared spectra of complexes **1** and **2** have in common peaks attributable to the presence of tren [two sharp (sh) and medium (m) intensity ν(N–H) stretching absorptions at 3290 and 3340 cm^{-1}] and unco-ordinated perchlorate [1080s (br) and 620m (sh)]. For **1** the presence of a single peak at 1640vs (sh) [ν_{asym}(OCO)], a doublet at 1350w and 1310m [ν_{sym}(OCO)] and another peak at 800m cm^{-1} [δ(OCO)] support the occurrence of bis(chelating) oxalate as observed by X-ray diffraction. In the spectrum of **2** a strong and broad feature in the region 3600–3100 cm^{-1} is indicative of the presence of strong hydrogen bonds. In addition the stretching C–O vibrations of squarate are located at 1730w, 1670w, 1610m and 1520s (br) cm^{-1}. The last feature is slightly split and corresponds to the strong and broad band at *ca.* 1500 cm^{-1} found in the spectrum of $K_2C_4O_4$.[20] The Ni–O (water) and Ni–O (squarate) bands are clearly detectable in the far-IR region (*ca.* 400 cm^{-1}).

The electronic spectra of complexes **1** and **2** as Nujol mulls, displaying maxima at 28 600, 18 080 and 10 600 (**1**) and at 28 170, 17 800 and 10 230 cm^{-1} (**2**), are consistent with a quasi-octahedral geometry around the nickel atom. A shoulder is also observed at *ca.* 16 400 cm^{-1} in both cases. On the basis of O_h symmetry, the maxima and the shoulder are assigned to transitions from the $^3A_{2g}$ ground state to $^3T_{1g}$ (P), $^3T_{1g}$ (F), $^3T_{2g}$ and ^1E_g excited states. The calculated values of 10*Dq* (ligand-field strength) and β (nephelauxetic ratio) are 10 600 cm^{-1} and 0.884 for **1** and 10 230 cm^{-1} and 0.896 for **2**. They are in the range normally found for octahedrally co-ordinated nickel(II) ions with an N_4O_2 chromophore.

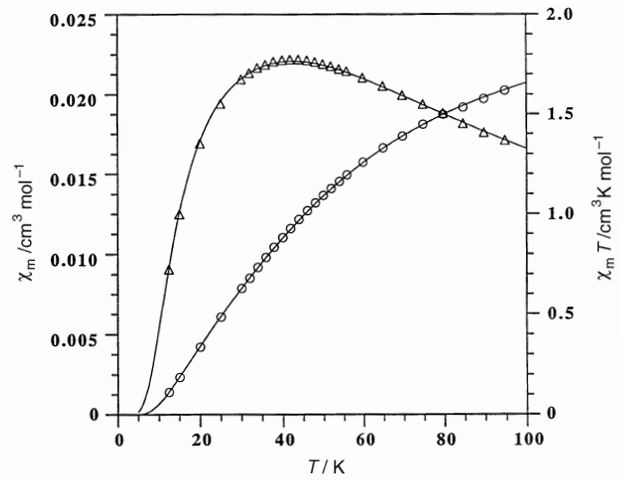

Fig. 4 Thermal dependence of the molar magnetic susceptibility (Δ) and $\chi_m T$ (o) for complex **1**. The solid lines correspond to the best theoretical fits (see text)

Magnetic properties

Plots of the magnetic susceptibility χ_m and $\chi_m T$ in the temperature range 100–12 K for complex **1** and 100–4.2 K for **2** are shown in Figs. 4 and 5, respectively. Both are characteristic of an antiferromagnetic interaction between the two single-ion triplet states. The value of $\chi_m T$ at room temperature is 1.89 cm^3 K mol^{-1} for **1** and 2.31 cm^3 K mol^{-1} for **2**. In the former case this value decreases on cooling and reaches a value of 0.11 cm^3 K mol^{-1} at 12 K (the susceptibility curve exhibits a maximum at 42.5 K indicating a relatively strong antiferromagnetic coupling). For complex **2** the value of $\chi_m T$ is constant until 30 K and decreases at lower temperatures reaching a value of 1.86 cm^3 K mol^{-1} at 4.2 K. In this case no susceptibility maximum is observed in the temperature range investigated. The intradimer exchange interaction (*J*) in dinuclear nickel(II) complexes can be treated with the isotropic spin Hamiltonian $\hat{H} = -J\hat{S}_A \cdot \hat{S}_B$ where $S_A = S_B = 1$ (local spins). The molar magnetic susceptibility for such a system is thus given by equation (1) where *N*,

$$\chi_m = \frac{2N\beta^2 g^2}{kT} \cdot \frac{\exp(J/kT) + 5\exp(3J/kT)}{1 + 3\exp(J/kT) + 5\exp(3J/kT)} \quad (1)$$

Table 3 Selected interatomic distances (Å) and angles (°) for compound **2** with e.s.d.s in parentheses

Nickel environment							
Ni(1)–O(1)	2.109(2)	Ni(2)–O(2)	2.143(2)	Ni(1)–N(12)	2.090(2)	Ni(2)–N(22)	2.099(2)
Ni(1)–O(1w)	2.055(2)	Ni(2)–O(2w)	2.095(2)	Ni(1)–N(13)	2.125(2)	Ni(2)–N(23)	2.096(2)
Ni(1)–N(11)	2.090(2)	Ni(2)–N(21)	2.073(2)	Ni(1)–N(14)	2.074(2)	Ni(2)–N(24)	2.083(2)
O(1)–Ni(1)–O(1w)	88.03(8)	O(2)–Ni(2)–O(2w)	91.74(7)	O(1w)–Ni(1)–N(14)	177.21(9)	O(2w)–Ni(2)–N(24)	171.89(8)
O(1)–Ni(1)–N(11)	172.40(8)	O(2)–Ni(2)–N(21)	177.43(9)	N(11)–Ni(1)–N(12)	96.69(9)	N(21)–Ni(2)–N(22)	94.9(1)
O(1)–Ni(1)–N(12)	90.29(8)	O(2)–Ni(2)–N(22)	82.54(8)	N(11)–Ni(1)–N(13)	92.51(9)	N(21)–Ni(2)–N(23)	94.9(1)
O(1)–Ni(1)–N(13)	80.00(8)	O(2)–Ni(2)–N(23)	87.55(8)	N(11)–Ni(1)–N(14)	84.43(9)	N(21)–Ni(2)–N(24)	83.48(9)
O(1)–Ni(1)–N(14)	93.33(9)	O(2)–Ni(2)–N(24)	95.90(8)	N(12)–Ni(1)–N(13)	163.54(9)	N(22)–Ni(2)–N(23)	163.36(9)
O(1w)–Ni(1)–N(11)	94.52(9)	O(2w)–Ni(2)–N(21)	88.76(9)	N(12)–Ni(1)–N(14)	84.1(1)	N(22)–Ni(2)–N(24)	83.67(9)
O(1w)–Ni(1)–N(12)	93.5(1)	O(2w)–Ni(2)–N(22)	94.65(9)	N(13)–Ni(1)–N(14)	83.28(9)	N(23)–Ni(2)–N(24)	84.10(9)
O(1w)–Ni(1)–N(13)	99.36(9)	O(2w)–Ni(2)–N(23)	98.99(8)				
Squarate ligand							
O(1)–C(1)	1.245(3)	O(3)–C(3)	1.257(3)	C(1)–C(2)	1.456(3)	C(2)–C(3)	1.469(3)
O(2)–C(2)	1.262(3)	O(4)–C(4)	1.254(3)	C(1)–C(4)	1.457(3)	C(3)–C(4)	1.450(3)
Ni(1)–O(1)–C(1)	144.2(2)	Ni(2)–O(2)–C(2)	126.4(2)	O(2)–C(2)–C(1)	134.5(2)	O(4)–C(4)–C(1)	133.3(2)
O(1)–C(1)–C(2)	138.0(2)	O(3)–C(3)–C(2)	134.6(2)	O(2)–C(2)–C(3)	135.9(2)	O(4)–C(4)–C(3)	136.4(2)
O(1)–C(1)–C(4)	131.8(2)	O(3)–C(3)–C(4)	135.4(2)	C(1)–C(2)–C(3)	89.6(2)	C(1)–C(4)–C(3)	90.3(2)
C(2)–C(1)–C(4)	90.2(2)	C(2)–C(3)–C(4)	90.0(2)				
tren ligand							
N(11)–C(11)	1.460(4)	N(21)–C(21)	1.461(4)	N(14)–C(16)	1.479(4)	N(24)–C(26)	1.473(4)
N(12)–C(13)	1.462(4)	N(22)–C(23)	1.485(4)	C(11)–C(12)	1.501(5)	C(21)–C(22)	1.512(5)
N(13)–C(15)	1.475(4)	N(23)–C(25)	1.467(4)	C(13)–C(14)	1.516(5)	C(23)–C(24)	1.502(5)
N(14)–C(12)	1.486(4)	N(24)–C(22)	1.491(4)	C(15)–C(16)	1.514(4)	C(25)–C(26)	1.504(5)
N(14)–C(14)	1.490(4)	N(24)–C(24)	1.482(4)				
Ni(1)–N(11)–C(11)	107.5(2)	Ni(2)–N(21)–C(21)	108.4(2)	C(14)–N(14)–C(16)	111.9(2)	C(24)–N(24)–C(26)	113.1(2)
Ni(1)–N(12)–C(13)	109.9(2)	Ni(2)–N(22)–C(23)	109.8(2)	N(11)–C(11)–C(12)	111.0(3)	N(21)–C(21)–C(22)	109.4(3)
Ni(1)–N(13)–C(15)	109.6(2)	Ni(2)–N(23)–C(25)	108.8(2)	N(14)–C(12)–C(11)	113.6(3)	N(24)–C(22)–C(21)	112.6(2)
Ni(1)–N(14)–C(12)	108.6(2)	Ni(2)–N(24)–C(22)	109.2(2)	N(12)–C(13)–C(14)	110.4(3)	N(22)–C(23)–C(24)	110.7(2)
Ni(1)–N(14)–C(14)	105.3(2)	Ni(2)–N(24)–C(24)	104.9(2)	N(14)–C(14)–C(13)	110.6(3)	N(24)–C(24)–C(23)	111.7(3)
Ni(1)–N(14)–C(16)	105.0(2)	Ni(2)–N(24)–C(26)	105.0(2)	N(13)–C(15)–C(16)	110.5(2)	N(23)–C(25)–C(26)	110.5(3)
C(12)–N(14)–C(14)	111.6(2)	C(22)–N(24)–C(24)	112.8(2)	N(14)–C(16)–C(15)	111.5(3)	N(24)–C(26)–C(25)	110.9(2)
C(12)–N(14)–C(16)	113.8(2)	C(22)–N(24)–C(26)	111.3(2)				

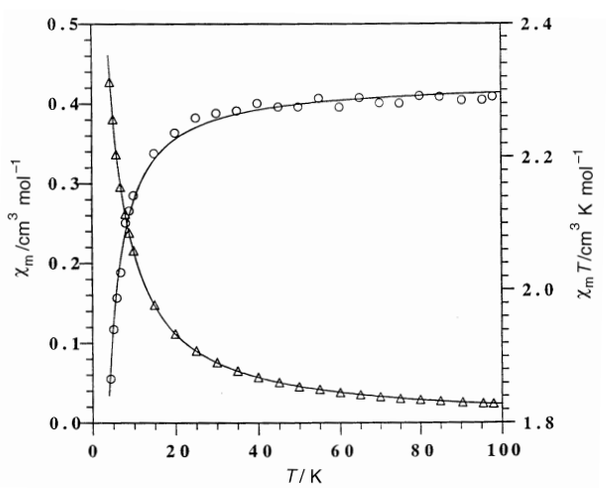

Fig. 5 Thermal dependence of the molar magnetic susceptibility (Δ) and $\chi_m T$ (o) for complex **2**. The solid lines correspond to the best theoretical fits (see text)

β, k, g and T have their usual meanings and it is assumed that $g_x = g_y = g_z$. Although nickel(II) in axial symmetry can have a large zero-field splitting, D, the magnetic behaviour of a nickel(II) dimer closely follows equation (1) when a relatively strong antiferromagnetic coupling is operative ($|J| \geqslant 20$ cm^{-1}).[21] This is the case for complex **1** where least-squares analysis of the experimental data using equation (1) led to $J = -28.8$ cm^{-1}, $g = 2.16$ and $R = 2.5 \times 10^{-5}$ {the agreement factor defined as $\Sigma_i[(\chi_m)_{obs}(i) - (\chi_m)_{calc}(i)]^2/\Sigma_i[(\chi_m)_{obs}(i)]^2$}. If the antiferromagnetic coupling is weak (complex **2**) or the coupling is ferromagnetic the effect of D has to be considered to describe the magnetic behaviour at low temperatures. The Hamiltonian to be used is then $\hat{H} = -J\hat{S}_A \cdot \hat{S}_B - D(\hat{S}_{ZA}^2 + \hat{S}_{ZB}^2)$. Thus, the least-squares analysis of the magnetic data for complex **2** through the corresponding theoretical expressions[21,22] yields $J = -0.38$ cm^{-1}, $g = 2.15$, $D = 1.7$ cm^{-1} and $R' = 1.12 \times 10^{-4}$ {defined as $\Sigma_i[(\chi_m)_{obs}T(i) - (\chi_m)_{calc}T(i)]^2/\Sigma_i[(\chi_m)_{obs}T(i)]^2$}. A similar quality of fit was obtained when the analysis of the magnetic data was done through equation (1) ($D = 0$), the values of J, g and R' being -0.4 cm^{-1}, 2.15 and 1.23×10^{-4}, respectively. As far as the magnetic coupling of complex **2** is concerned, the values obtained through the two approaches are small and very similar. Finally, when J was assumed to be zero and D and g were the variable parameters the results of the fit were $D = 5.7$ cm^{-1}, $g = 2.13$ and $R' = 1.17 \times 10^{-4}$. In the light of these results concerning complex **2**, it is clear that the maximum value of the antiferromagnetic exchange coupling is -0.4 cm^{-1} and that the value of D can vary between zero and 5.7 cm^{-1}. Anisotropic measurements on single crystals are required to determine accurately the value of D.

The value of $-J$ for complex **1** (28.8 cm^{-1}) is practically identical to that (28.9 cm^{-1}) reported[10j] for the complex $[Ni_2(C_2O_4)L_2][ClO_4]_2 \cdot 2H_2O$ where L is *N*,*N*′-bis(3-aminopropyl)ethane-1,2-diamine, and in the lower limit of the range observed for oxalato-bridged dinuclear nickel(II) complexes with an NiN_4O_2 chromophore[10k] (maximum $-J$ 39 cm^{-1}). The distortions of the octahedral symmetry around the metal ion in **1** [Ni–N(tren) distances ranging from 2.145(3) to 2.057(4) Å and Ni–O (oxalate) 2.112(2) and 2.049(2) Å] account for the slight weakening of the observed antiferromagnetic coupling. It is well known that the exchange pathway in this oxalato-bridged family involves overlap between the equatorial $d_{x^2-y^2}$

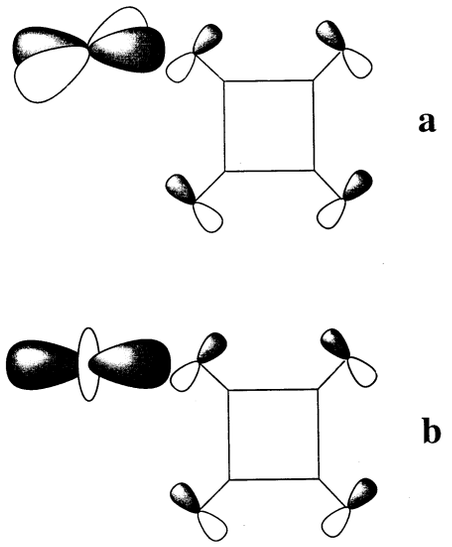

Scheme 1

magnetic orbitals of the nickel atoms [the *x* and *y* axes are roughly defined by the Ni–O (oxalate) bonds] and the symmetry-adapted highest occupied molecular orbitals (HOMOs) of the oxalate ligand. Consequently, differences in the bond lengths around metal ions with the same chromophore are directly related to the overlap between the $d_{x^2-y^2}$ magnetic orbitals and thus affect the magnitude of the antiferromagnetic coupling.

The magnetic coupling in complex **2** is also antiferromagnetic but very weak (*J ca.* -0.4 cm^{-1}). In this case the overlap between two $d_{x^2-y^2}$ magnetic orbitals of the nickel atoms [the Ni(1)–O(1) and Ni(1)–O(1w) bonds define the *x* and *y* axes around Ni(1), whereas Ni(2)–O(2) and Ni(2)–O(2w) correspond to the *x* and *y* axes around Ni(2)] occurs through the extended OCCO squarate fragment [Ni(1) ··· Ni(2) 6.224(1) Å] and is expected to be very poor. In fact the magnetic coupling between two copper(II) ions with the same type of squarato bridge, where the orbital on each magnetic centre is also of the $d_{x^2-y^2}$ type, is -10.3 cm^{-1}.[23] In order to understand this lowering of the antiferromagnetic coupling when going from Ni^{II} to Cu^{II} one must consider that the experimental *J* parameter can be decomposed into a sum of individual contributions, $J_{\mu\nu}$, from each pair of magnetic orbitals involved in the exchange phenomenon [equation (2)],[24] where n_A and n_B are the number

$$J = 1/n_A n_B \sum_{\mu=1}^{n_A} \sum_{\nu=1}^{n_B} J_{\mu\nu} \qquad (2)$$

of unpaired electrons localized on the metal ions A and B. This equation shows that the magnitude of the net antiferromagnetic interaction is properly described by $n_A n_B J$ and not by *J*. The value of $n_A n_B J$ is -1.6 cm^{-1} for **2** and -10.3 cm^{-1} for the related copper(II) complex. Given that the metal–metal separation through squarate-O^1,O^3 is larger than 6 Å, the ferromagnetic terms are expected to be negligible and equation (2) reduces to (3). At this stage, it should be noted that the values of $n_A n_B J$

$$n_A n_B J \approx J_{x^2-y^2,\ x^2-y^2} \qquad (3)$$

in equation (2) are based on the assumption that the energy of the 3d magnetic orbitals is the same independently of the type of metal under consideration. It is clear that the energy of the 3d orbitals increases when going from Cu^{II} to Ni^{II} and thus the energy gap between the $d_{x^2-y^2}$ magnetic orbital and the symmetry-adapted HOMOs of the squarato bridge becomes larger for Ni^{II}. This causes a poorer overlap between the magnetic orbitals through the bridge in the nickel(II) as compared to the copper(II) complex, and leads to a smaller $-J_{x^2-y^2,\ x^2-y^2}$ value as observed.

The value of *J* for the squarate-O^1,O^2-bridged nickel(II) complex $[Ni(C_4O_4)(bipy)(H_2O)_2]\cdot 2H_2O$[12] is -1.7 cm^{-1}. This contrasts with the much weaker coupling observed for **2** (-0.4 cm^{-1}). A comparison of the magnetic orbitals responsible for the magnetic coupling in these two squarate-O^1,O^3-bridged nickel(II) complexes clarifies this apparent anomaly. Their crystal structures show that the magnetic orbital which points toward the squarato bridge is of the $d_{x^2-y^2}$ type in **2** and d_{z^2} in the bipy derivative. These magnetic orbitals of the hypothetical monomeric fragments of both compounds are shown in Scheme 1. Simple orbital considerations lead to a ratio $S_{b,b'}/S_{a,a'}$ equal to $\frac{4}{3}$ where *S* represents the overlap integral between the two magnetic orbitals, a and a′ (compound **2**) or b and b′ (bipy compound) in the dimer.[25] Given that in the framework of Kahn's orbital model[26] *J* varies as S^2 (one electron per magnetic centre), the relative magnitude of the antiferromagnetic interaction is predicted to be 16/9. Keeping in mind that the antiferromagnetic coupling is -1.7 cm^{-1} for the bipy compound and that this value has to be considered as a maximum because factors such as the zero-field splitting were neglected in its estimation, our prediction is a maximum of -1 cm^{-1} for the magnetic coupling for **2**. This is quite good in spite of the crude orbital model used and in the lack of a more accurate value for *J* for the bipy compound.

Acknowledgements

Financial support from the Dirección General de Investigación Científica y Técnica (DGICYT) (Spain) through Project PB94-1002 is gratefully acknowledged.

References

1 M. Verdaguer, M. Julve, A. Michalowicz and O. Kahn, *Inorg. Chem.*, 1983, **22**, 2624.
2 M. Habenschuss and B. C. Gerstein, *Chem. Phys.*, 1974, **61**, 852.
3 X. Solans, M. Aguiló, A. Gleizes, J. Faus, M. Julve and M. Verdaguer, *Inorg. Chem.*, 1990, **29**, 775.
4 D. L. Kepert, in *Inorganic Stereochemistry*, eds. C. K. Jørgensen, M. F. Lappert, S. J. Lippard, J. L. Margrave, K. Niedenzu, H. North, R. W. Parry and H. Yamatera, Springer, Berlin, 1982, vol. 6.
5 C. Robl and A. Weiss, *Z. Naturforsch., Teil B*, 1986, **41**, 1490; C. Robl, V. Gnutzmann and A. Weiss, *Z. Anorg. Allg. Chem.*, 1987, **549**, 187; C. Robl and A. Weiss, *Mater. Res. Bull.*, 1987, **22**, 373.
6 J. C. Trombe, J. F. Petit and A. Gleizes, *New J. Chem.*, 1988, **12**, 197; *Inorg. Chim. Acta*, 1990, **167**, 69; *Eur. J. Solid State Inorg. Chem.*, 1991, **28**, 669.
7 D. Coucouvanis, F. J. Hollander, R. West and D. Eggerding, *J. Am. Chem. Soc.*, 1974, **96**, 3006; D. Coucouvanis, D. G. Holah and F. J. Hollander, *Inorg. Chem.*, 1975, **14**, 2657.
8 M. L. Calatayud, I. Castro, J. Sletten, J. Cano, F. Lloret, J. Faus, M. Julve, G. Seitz and K. Mann, *Inorg. Chem.*, 1996, **35**, 2858.
9 R. Grenz, F. Götzfreid, U. Nagel and W. Beck, *Chem. Ber.*, 1986, **119**, 1217.
10 (*a*) P. W. Ball and A. B. Blake, *J. Chem. Soc.*, 1969, 1415; (*b*) D. M. Duggan, E. K. Barefield and D. N. Hendrickson, *Inorg. Chem.*, 1973, **12**, 985; (*c*) V. V. Zelentsov, L. M. Chanturiya and N. I. Pitskhalava, *Koord. Khim.*, 1978, **4**, 764; (*d*) J. Ribas, M. Monfort, C. Díaz and X. Solans, *An. Quím.*, 1988, **84**, 186; (*e*) L. P. Battaglia, A. Bianchi, A. Bonamartini Corradi, E. García-España, M. Micheloni and M. Julve, *Inorg. Chem.*, 1988, **27**, 4174; (*f*) A. Bencini, A. Bianchi, P. Paoli, E. García-España, Y. Jeannin, M. Julve, V. Marcelino and M. Philoche-Levisalles, *Inorg. Chem.*, 1990, **29**, 963; (*g*) A. Bencini, A. Bianchi, P. Paoli, E. García-España, M. Julve and V. Marcelino, *J. Chem. Soc., Dalton Trans.*, 1990, 2213; (*h*) K. Yamada, Y. Fukuda, T. Kawamato, Y. Kushi, W. Mori and K. Unuora, *Bull. Chem. Soc. Jpn.*, 1993, **66**, 2758; (*i*) A. Escuer, R. Vicente, J. Ribas, J. Jaud and B. Raynaud, *Inorg. Chim. Acta*, 1994, **216**, 139; (*j*) A. Escuer, R. Vicente, M. Sallah El Fallah and J. Jaud, *Inorg. Chim. Acta*, 1995, **232**, 151; (*k*) P. Román, C. Guzmán-Miralles, A. Luque, J. I. Beitia, J. Cano, F. Lloret, M. Julve and S. Alvarez, *Inorg. Chem.*, 1996, **35**, 3741.

11 J. A. C. van Ooijen, J. Reedijk and A. L. Spek, *Inorg. Chem.*, 1979, **18**, 1184.
12 R. Soules, F. Dahan, J. P. Laurent and P. Castan, *J. Chem. Soc., Dalton Trans.*, 1988, 587.
13 A. Earnshaw, *Introduction to Magnetochemistry*, Academic Press, London, New York, 1968.
14 P. Main, S. J. Fiske, S. E. Hull, L. Lessinger, G. Germain, J. P. DeClercq and W. W. Woolfson, MULTAN 80, A System of Computer Programs for the Automatic Solution of Crystal Structures from X-Ray Diffraction Data, University of York, 1980.
15 C. K. Fair, MOLEN, An Interactive Structure Solution Procedure, Enraf-Nonius, Delft, 1990.
16 D. T. Cromer and J. T. Waber, *International Tables for X-Ray Crystallography*, Kynoch Press, Birmingham, 1974, vol. 4, Table 2.2.B; D. T. Cromer and J. B. Mann, *Acta Crystallogr., Sect. A*, 1968, **24**, 321.
17 D. T. Cromer, *International Tables for X-Ray Crystallography*, Kynoch Press, Birmingham, 1974, vol. 4, Table 2.3.1.
18 (*a*) P. D. Cradwick and D. Hall, *Acta Crystallogr., Sect. B*, 1970, **26**, 1384; (*b*) D. M. Duggan and D. N. Hendrickson, *Inorg. Chem.*, 1974, **13**, 2056; (*c*) C. G. Pierpont, D. N. Hendrickson, D. M. Duggan, F. Wagner and E. K. Barefield, *Inorg. Chem.*, 1975, **14**, 604; (*d*) B. C. Segal and S. J. Lippard, *Inorg. Chem.*, 1977, **16**, 1623; (*e*) C. G. Pierpont, L. C. Francesconi and D. N. Hendrickson, *Inorg. Chem.*, 1977, **16**, 1977.
19 D. Semmingsen, *Acta Chem. Scand.*, 1973, **27**, 3961.
20 M. Ito and B. West, *J. Am. Chem. Soc.*, 1963, **85**, 2580.
21 G. De Munno, M. Julve, F. Lloret and A. Derory, *J. Chem. Soc., Dalton Trans.*, 1993, 1179.
22 A. P. Ginsberg, R. L. Martin, R. W. Brookes and R. C. Sherwood, *Inorg. Chem.*, 1972, **11**, 2884.
23 C. E. Xanthopoulos, M. P. Sigalas, G. A. Katsoulos, C. A. Tsipis, C. C. Hadjikostas, A. Terzis and M. Mentzafos, *Inorg. Chem.*, 1993, **32**, 3743.
24 O. Kahn, *Struct. Bonding* (*Berlin*), 1987, **68**, 89 and refs. therein.
25 I. Castro, J. Sletten, M. L. Calatayud, M. Julve, J. Cano, F. Lloret and A. Caneschi, *Inorg. Chem.*, 1995, **34**, 4903.
26 O. Kahn and M. F. Charlot, *Nouv. J. Chim.*, 1980, **4**, 567.

Received 5*th September* 1996; *Paper* 6/06105B